

VLEO2025-5-03

# Air-breathing Electric Propulsion: Testing Approaches and Simulations

Bruno MORICONI<sup>1</sup>, Vittorio GIANNETTI<sup>1</sup>, Eugenio FERRATO<sup>1</sup>, and Tommaso ANDREUSSI<sup>1</sup>

<sup>1</sup>*Institute of Mechanical Intelligence, Sant'Anna School of Advanced Studies*

Contact: bruno.moriconi@santannapisa.it

## Abstract

Air-breathing electric propulsion combines an air intake with an electric thruster to collect and accelerate the atmospheric particles in front of the spacecraft. Collecting the propellant from the atmosphere could enable long-duration space missions at very low altitudes, but the complexities of reproducing on-ground an environment representative of VLEO hindered the development and the technological maturation of the concept. In the framework of the BREATHE ERC project, a novel strategy for the characterization of air-breathing propulsion is being developed, merging experiments with modeling and simulations. This work highlights the design of the BREATHE facility and the development of a numerical suite to simulate the main physical processes of atmospheric neutral flows.

**Key words:** Air-breathing electric propulsion, Vacuum facility, Rarefied gas dynamics, Numerical simulations, Ground testing

## 1. Introduction

Air-breathing electric propulsion (ABEP) combines an air intake with an electric thruster to collect and accelerate the atmospheric particles. The realization of air-breathing thrusters capable of compensating the drag acting on the spacecraft may allow for extended space missions operating at significantly lower altitudes. Operating in very-low Earth orbits (VLEOs), below 400 km, offers significant advantages, such as improved performance for observation and telecommunication payloads, as well as promoting more sustainable space utilization through enhanced orbit accessibility and accelerated space debris decay. Despite these benefits, the technological maturity of the ABEP concept remains limited. Efforts to validate the complete drag compensation capabilities of the ABEP systems have been hampered by the challenges of replicating a representative VLEO environment on-ground. Consequently, numerous research initiatives have concentrated on independently analysing and testing the intake and thruster components [1], avoiding the complexities of recreating VLEO flows. The intake performance is typically analysed using Direct Simulation Monte Carlo (DSMC) methods, allowing the estimation of the flow conditions at the thruster inlet, in terms of particle density, composition and flow rate. The thruster operation and performance are then measured through stand-alone testing, directly feeding the thruster with atmospheric propellant. Despite the effectiveness of this simplified approach in assessing the concept feasibility, the separate analysis of thruster and intake hides some critical aspects of the opera-

tion of the full ABEP system. The first limitation is the low accuracy in predicting intake performance, due to uncertainties in the interactions between rarefied flow particles and the intake walls, as well as the time evolution of these interactions. Moreover, the level of inaccuracy is further increased for those ABEP systems in which the collection and ionization regions significantly overlap. From the experimental point of view, the direct feeding approach obscures the measurement of the thruster's transmission probability, i.e. the probability that a particle entering the thruster reaches the thruster exhaust, and its dependence on the system operating conditions. At the time of writing the present article, only three institutions - Busek, JAXA, and SITAEL - have conducted on-ground end-to-end testing of the ABEP technology [1], but none of the systems has demonstrated the capability to ensure full drag compensation.

The ongoing efforts at the Sant'Anna School of Advanced Studies, in the framework of the BREATHE ERC project, aim at developing the ABEP system and verifying its drag compensation capabilities by means of an alternative on-ground testing approach. This approach aims at recreating on-ground VLEO orbital conditions and developing modeling and simulation tools, allowing for the identification of scaling laws of ABEP processes to miniaturize the system at CubeSat scale.

The present paper describes in Sec. 2 the approach for verifying ABEP system functionality. After an overview of the VLEO environment, the section elaborates on the BREATHE verification strategy and on

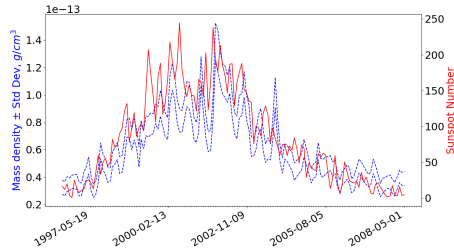


**Figure 1: Space-averaged mass density and solar activity during the 23rd solar cycle at 250 km altitude.**

the dedicated vacuum facility tailored for the project. Sec. 3 summarizes the conclusions of the paper and the outcomes of performed activities.

## 2. Methodology

In Sec. 2.1, the expected environmental conditions in VLEO are presented. Subsequently, Sec. 2.2 and Sec. 2.3 detail the strategy employed for air-breathing thruster verification in the framework of the BREATHE project and the BREATHE vacuum facility.

### 2.1. VLEO environment

VLEO orbits are defined as Earth orbits with a mean altitude in the range of 100 km to 450 km [1]. The operation and performance of an ABEP system in VLEO are related to the properties of the atmosphere collected by the intake, in terms of composition, density, temperature, and asymptotic velocity. These parameters change depending on the altitude of the spacecraft, the Earth’s climate and the solar activity. As an example, Fig. 1 depicts the variation of the space-averaged total mass density at 250 km altitude during the 23rd solar cycle within a standard deviation, together with the solar activity. Building upon [2], averaged number densities for each species are evaluated using the NRLMSISE-00 atmospheric model and used as input in the mathematical model described in Sec. 2.3.1 with 30 days temporal resolution, 10 degrees latitude, 30 degrees longitude. Table 1 reports the mean number densities of the species for the reference altitudes of 200 km, 250 km and 300 km, in good agreement with those obtained in [3]. The main constituents of the atmosphere in VLEO are molecular nitrogen, atomic oxygen and molecular oxygen, characterized by relatively low densities. This aspect poses additional challenges to be tackled for the operation of an ABEP system in VLEO: material compatibility and efficient operation. Indeed, the former implies severe constraints for materials due to the degradation associated with the presence of atomic oxygen. For the latter, nitrogen and oxygen have higher first ionization energy, lower electron ionization cross section

and lower mass with respect to xenon, the typical propellant used in plasma thrusters. Table 2 reports some reference values for molecular nitrogen, atomic oxygen [4] and xenon [5].

### 2.2. BREATHE Verification Strategy

In the framework of the BREATHE project, three main activities are planned: the development of a virtual laboratory to simulate the ABEP behavior in orbit and the analysis of the mission during thruster operation; the creation of a facility capable of reproducing on-ground VLEO conditions in a representative manner in terms of number density and mass flow rate at the thruster entrance; the design, building and testing of different prototypes, investigating multiple combinations of ionization and acceleration mechanisms to identify scaling laws of the ABEP system.

The setup for reproducing VLEO on-ground involves the design of a novel vacuum facility, which will allow to characterize the thruster transmissivity and assess its dynamic behavior in air-breathing conditions, as described in Sec. 2.3. A qualitative representation of the experimental setup is shown in Fig. 2, highlighting also its equivalence with the thruster in-orbit operation. Once the satellite is deployed in orbit, the intake functions as a molecular trap for the rarefied flow, increasing the particle number density at the ionization region and reducing the flow of the collected atmosphere that leaves the thruster without crossing the ionization and acceleration regions. In this collection process, only a small fraction of particles cross the intake and the thruster experiencing no collisions, while the majority of neutral particles are scattered by collisions with the walls or ionized by the thruster. Similarly, this condition can be reproduced on-ground with a propellant distributor that injects the exact flow of simulating VLEO propellant collected downstream the intake while in orbit. On the other hand, the backflow is simulated through an outlet equipped with a turbomolecular pump with tunable pumping speed, providing an independent control on the thruster pressure. The other outlet will correspond to the thruster exhaust. The pressure in the propellant distributor of the facility will vary according to the propellant flow rate injected and the pumping speed of the turbomolecular pump. By closing the thruster outlet, the dependence of the pressure on the flow rate and the pumping speed of the turbomolecular pump can be characterized. Then, during thruster operation, the measurement of the distributor backpressure will allow to assess the flux through the thruster outlet and, consequently, the fraction of propellant processed. This aspect is the main innovation of the verification approach proposed. Indeed, when a thruster is pipe-fed via a mass flow regulator a linear relation between the injected mass flow and the gas pressure holds, resulting in conditions not representative of thruster operation in air-breathing mode.

**Table 1: Averaged Earth atmospheric composition from NRLMSISE-00**

Number density, $1e16/m^3$	200km	250km	300km
$N_2$	0.32	0.057	0.013
$O$	0.37	0.131	0.053
$O_2$	0.016	0.0022	0.00037

**Table 2: Ionization and mass properties for species of interest**

Species	Ionization energy, eV	Ionization cross-section ( $cm^2$ )	Weight, amu
$Xe$	12.13	5e-16	131
$O$	13.62	1.5e-16	16
$N_2$	15.58	2.5e-16	28

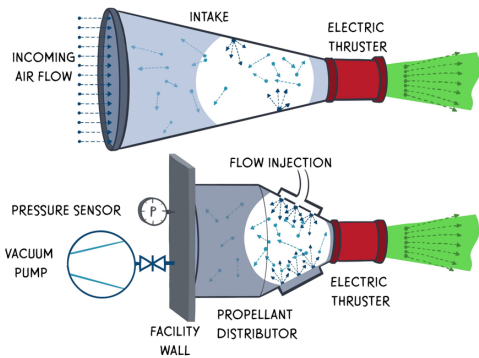


**Figure 2: Schematic representation of intake flow compression (top) and the setup for transmissivity testing (bottom).**

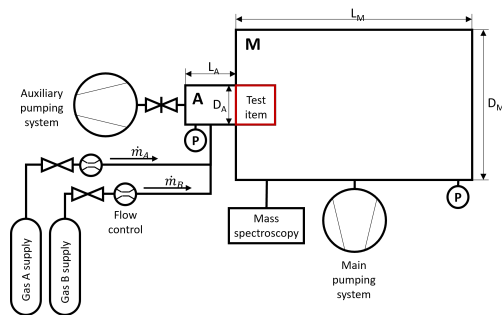


**Figure 3: Schematics of the BREATHE facility.**

### 2.3. BREATHE Vacuum Facility

As depicted in Fig. 3, the BREATHE facility comprises a main chamber (M) and an auxiliary chamber (A), both featuring dedicated pumping systems. A throttle valve is inserted in the auxiliary chamber, in front of the turbomolecular pump, to regulate the pumping speed. The equipment under test (i.e., the open-inlet air-breathing thruster) will be placed at the interface between the two chambers. By independently regulating the injected mass flow rate and the pressure difference between the two chambers, it will be possible to fine tune the flow properties (in terms of particle flux and pressure) inside the thruster control volume, and thus achieve a good level of representa-

tiveness of thruster operation in air-breathing mode. A control system manages two distinct gas supplies ( $N_2$  and a  $N_2/O_2$  mixture or  $N_2/Ar$  mixture), monitors the space simulator and to controls the pumping system. After flow regulation and mixing, the supplied gases are injected in the auxiliary chamber and diffuse into the main vessel through the test item. The possibility to independently regulate the injected mass flow rate and the pressure difference between the two chambers is used to characterize the test item in terms of its transmission probability of the rarefied gas flows.

The lack of a PFG in the BREATHE facility will not allow the characterization of particle collection and the analysis of atomic oxygen effects, e.g., hiding the aspects associated with material degradation. Concerning the propellant representativeness, argon will be used as a surrogate thanks to its similarities with the atomic oxygen present in the higher atmosphere [1], [6]. The effects of atomic oxygen on material compatibility will be investigated during the thruster prototypes development phase, exploiting the dissociation of molecular oxygen in the thruster discharge.

#### 2.3.1. Analysis of Facility Performance

A preliminary assessment of the facility capability to simulate VLEO conditions inside the thruster has been performed via a 0D model in [7] and further extended in the present work to assess the chamber representativeness in a wider range of conditions. Two particle flow balances are derived, corresponding to in-flight conditions in the air-breathing system and to on-ground conditions in the auxiliary chamber. For both balances, the assumptions made follow the model developed in [8], i.e., free molecular flow, single species ideal gas modeled through weighted average properties at 200 km (from Table 1 and Table 2), fully diffusive reflection after wall collisions, fixed wall temperature and only thermal mass flux with no macroscopic velocity upstream the thruster. The particle flow continuity equation for the thruster control volume is written in Eq. 1

$$V \frac{\partial N}{\partial t} = \dot{N}_{In} - N v_{Th}^O [A_{Bf} \Theta_{Bf} + A_{Th} \Theta_{Th}] \quad (1)$$

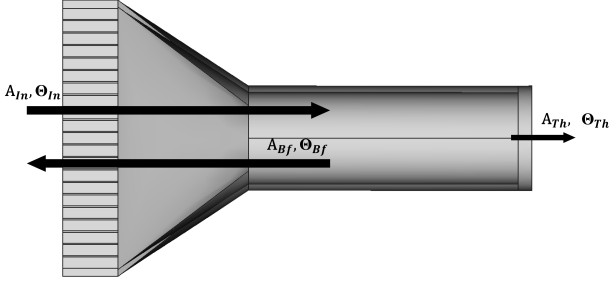


**Figure 4: Thruster geometry considered for the 0D model particle flow balance.**

where  $\dot{N}_{In}$  is obtained from Eq. 2

$$\dot{N}_{In} = n_{\infty} v_{\infty} A_{In} \Theta_{In} \quad (2)$$

with  $n_{\infty}$ ,  $v_{\infty}$  corresponding to the asymptotic number density and velocity,  $A_{In}$  the intake area and  $\Theta_{In}$  the transmission probability at the thruster inlet. In Eq. 1, the first term on the right represents the incoming asymptotic flow accepted by the intake, the second term corresponds to the backflow of thermalized particles toward the intake, and the last term is the flow of thermalized particles leaving the thruster.  $N$  is the particle number density in the thruster ionization chamber control volume,  $A_{Bf}$  is the thruster backflow area,  $\Theta_{Bf}$  is the backflow transmission probability through the intake,  $V$  represents the volume and  $A_{Th}$  and  $\Theta_{Th}$  are the thruster outlet area and transmission probability, respectively. With the considered set of hypotheses, the molecule's velocity along a specific direction can be deduced considering that in an equilibrium gas only half of the molecules will have a positive component of velocity along a specific axis [9], therefore

$$v_{Th}^O = \sqrt{\frac{k_B T_W^O}{2\pi m_p}} \quad (3)$$

with  $T_W^O$  being the temperature of the thruster walls in orbit (fixed at 400 K),  $k_B$  the Boltzmann constant and  $m_p$  the mass of the species. Fig. 4 depicts the thruster geometry considered, which mainly consists of a squared entrance of 10 cm side length with equally spaced squared holes separated by a wall of 0.5 mm thickness, transitioning via a lofted square-based cone into a circular cross-section with a radius of 3 cm. The total length of the intake is fixed to 7 cm. The dimensions have been selected to fit the ABEP system in a 2U CubeSat.

In the framework of this preliminary analysis, an estimation of the intake transmission probabilities has been performed combining transmittance values for cylindrical ducts with those for conical orifices. Indeed, in [10] and [11] it is interestingly shown that the exact shape of the duct cross-section has no significant

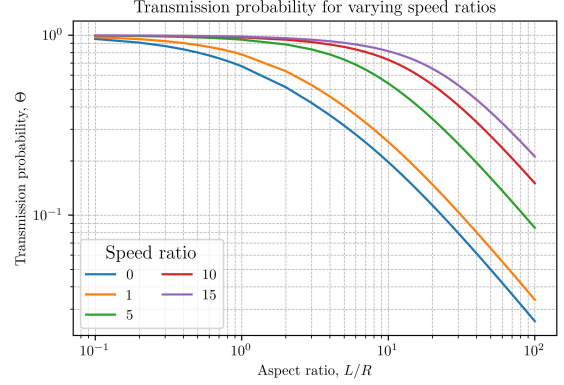


**Figure 5: Transmission probabilities through cylinders of different aspect ratios and velocity entrance with zero angle of attack.**

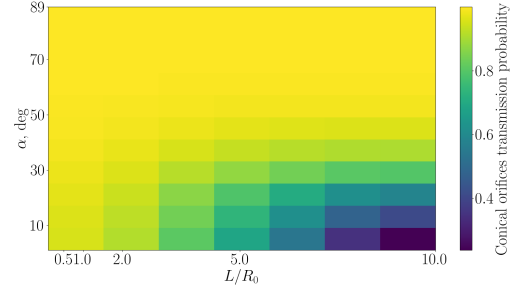


**Figure 6: Transmission probabilities for conical orifices.**

effect on the overall transmission probability. A duct with a circular section leads to the highest beam transmission probability, but the decrease of transmission probability for any regular polygonal tube is within 2.8 % at maximum for aspect ratios lower than 100. Therefore, the squared ducts are modeled as cylindrical ones with the same cross-sectional area and the same length. From [12] the transmission probabilities for cylindrical ducts with arbitrary speed ratio  $S$  and zero angle of attack is computed, where  $S$  is obtained from Eq. 4,

$$S = \frac{u}{\sqrt{2k_B T_{\infty}/m_p}} \quad (4)$$

with  $T_{\infty}$  is the asymptotic temperature. The results of the approach described in [12] are qualitatively shown in Fig. 5. The honeycomb structure filled with squared holes is followed by a cone transitioning from a squared base to the circular thruster entrance. The reference paper for the solution of the transmission probability for conical orifices is [13]. The authors solve the problem of evaluating numerically the flow transmission probability in both directions through conical orifices of any lengths and angles. The transmission probability for a molecule going from the smaller face of the cone to the larger face is qualitatively depicted in Fig. 6. The probability of transmission for a molecule passing from the larger end to the smaller end is ob-

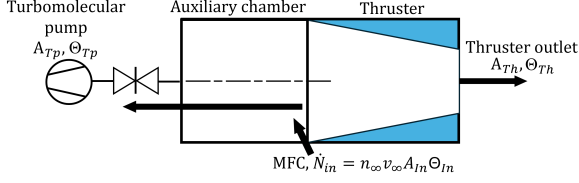


Figure 7: Auxiliary chamber setup.

tained considering that, as the authors of [13] suggest, for two vessels containing gas at equal pressures and separated by a cone-shaped orifice, the number of molecules moving from the first container to the second must be exactly balanced by the number of molecules moving from the second to the first.

Downstream the honeycomb, the intake has been modeled as a cone with an area of aperture on the honeycomb side equivalent to the opening area of the intake. The total transmission probability of the intake has then been evaluated in the following steps. The total transmittance of the honeycomb entrance, made from many straws, is evaluated as the single cylinder transmittance multiplied by the ratio between the sum of the cross-sectional areas of the straws to the total inlet area. For the lofted cone side, solutions from [13] have been used. The values of the obtained transmittances have then been combined as in [14] for the adjoining honeycomb ducts and cone. This procedure led to the evaluation of  $\Theta_{IC}$  and  $\Theta_{Bf}$  for different cone length and intake opened area, the latter changed by varying the number of squared holes.

In the auxiliary chamber mass flow controllers (MFC) inject the mixture with a mass flow rate mimicking the one experienced in orbit by the satellite after the intake collection, see Fig. 7. The particle flow balance is therefore written as in Eq. 5

$$V \frac{\partial N}{\partial t} = \dot{N}_{in} - v_{th}^{Ch} N [A_{Tp} \Theta_{Tp} + A_{Th} \Theta_{Th}] \quad (5)$$

where, in this case,  $v_{th}^{Ch}$  represents the molecule's velocity along a specific direction corresponding to the chamber walls temperature,  $T_W^{Ch}$ . For a fixed pumping speed  $S_{l/s}$  (in liters per second), the product  $A_{Tp} \Theta_{Tp}$  between the collecting area of the turbomolecular pump and the transmission through the turbomolecular pump is estimated as in Eq. 6

$$A_{Tp} \Theta_{Tp} = \sqrt{\frac{2\pi m_p}{k_B T_W^{Ch}}} \cdot 10^{-3} S_{l/s} \quad (6)$$

Comparing Eq. 5 and Eq. 1 it is seen that, by properly tuning the pumping speed of the pump, it is possible to reproduce in the auxiliary chamber the same conditions experienced by the satellite in orbit after the intake collection, by equating as in Eq. 7

$$S_{l/s} = A_{Bf} \Theta_{Bf} v_{th}^O 10^3 \quad (7)$$

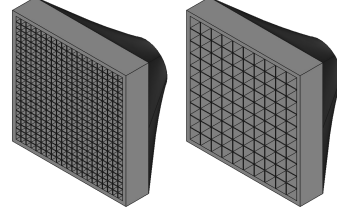


Figure 8: Intake configurations example.

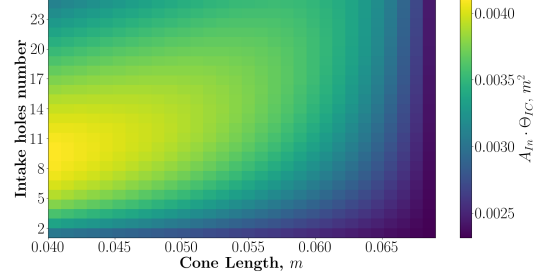


Figure 9:  $A_{In} \Theta_{IC}$  variation for different cone length and intake area.

which is derived from the imposition of Eq. 8

$$v_{th}^O A_{Bf} \Theta_{Bf} = v_{th}^{Ch} A_{Tp} \Theta_{Tp} \quad (8)$$

The tuning of the pumping speed allows for the investigation of a wide range of intake transmittances and in principle will allow to assess the variability of the thruster transmittance by accurately probing the pressure in the chamber. To show this, the number of equally spaced squared holes on the intake has been varied from 1 to 25, preserving a constant wall thickness of 0.5 mm. A smaller number of holes leads to a larger intake collecting area, without impacting the selected cone length. An example of this approach is depicted in Fig. 8, showing two different intake with the same cone length but different opened area. Several cone length have been analysed, from 4 cm to 6.5 cm, with a step of 1 mm. The variation of the cone length impacts not only the transmission of the cone itself but also the aspect ratio of the squared holes. In all the configurations analysed, the total length of the intake, made by the adjoining honeycomb and conical sections, was fixed to 7 cm.

The following figures summarize the obtained results. Fig. 9 depicts the variability of  $A_{In} \cdot \Theta_{IC}$ , Fig. 10 shows the transmission probability at the thruster entrance,  $\Theta_{IC}$ , and Fig. 11 the reverse flow transmission probability from the thruster entrance,  $\Theta_{Bf}$ , for different cone length and intake area. From Fig. 11 it is possible to evaluate the pumping speed of the turbomolecular pump for the different conditions. The result of this is reported in Fig. 12, showing the pumping speed necessary to ensure the same number density in the thruster ionization chamber as the orbital one after the intake collection. The number density

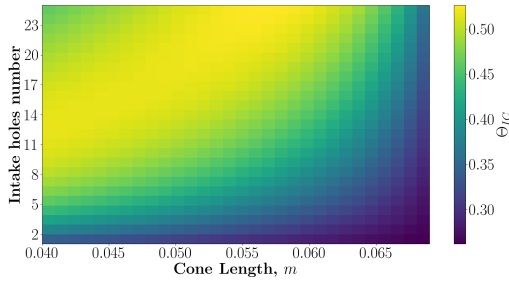


Figure 10:  $\Theta_{IC}$  variation for different cone length and intake area.

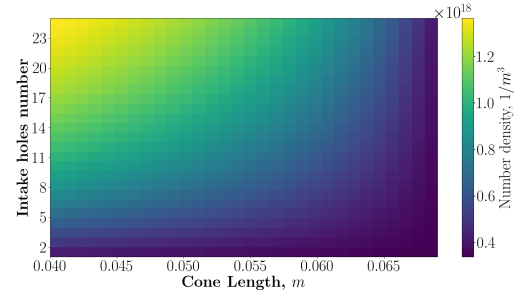


Figure 13: Number density variation for different cone length and intake area.

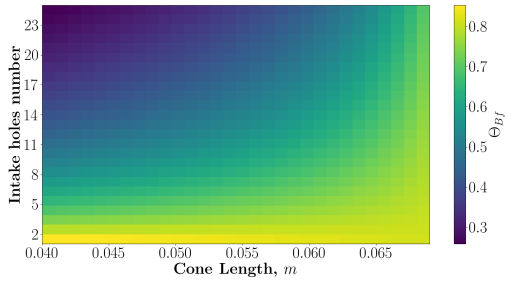


Figure 11:  $\Theta_{Bf}$  variation for different cone length and intake area.

estimated for the different configurations are qualitatively shown in Fig. 13, considering a  $\Theta_{Th} = 0.3$  and  $A_{Th} = 1.8 \cdot 10^{-4} \text{ m}^2$ .

As expected, when the intake backflow transmission probability is higher, the collection and compression of gas is less efficient, therefore a lower pressure and particle number density is available in the thruster. Thus, a higher pumping speed of the turbomolecular pump is required to finely tune the pressure inside the auxiliary chamber.

The estimated values of number densities and pumping speed for the different intake configurations contain inaccuracies associated with the assumptions made, but demonstrate the representativeness and feasibility of the proposed testing approach, as they will be equally achievable both in orbit and in the auxiliary chamber setup.

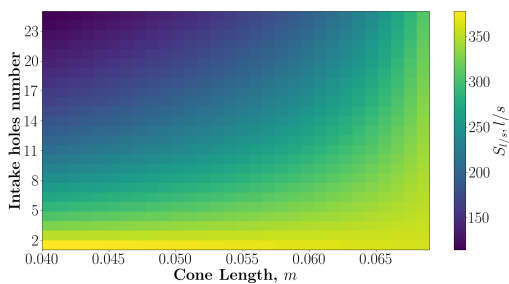


Figure 12:  $S_{I/s}$  variation for different cone length and intake area.

### 3. Conclusions

In recent years, as the benefits of operating in VLEO become increasingly evident, the development of ABEP systems has garnered significant attention from research institutions and space industries. Testing and validating ABEP systems on-ground remain critical challenges, requiring specialized facilities capable of reproducing representative flow conditions. This work highlights a novel approach being developed to address these challenges. Within the BREATHE project, an innovative setup independently regulates the injected mass flow rate and thruster inlet pressure, achieving a high level of representativeness for air-breathing mode operation. This approach enables dynamic testing under varying input conditions, probing the thruster's behavior at low densities and measuring its transmission probability across a range of operating conditions. The BREATHE laboratory will provide an innovative and efficient platform for on-ground characterization of air-breathing thrusters once operational.

### Acknowledgments

The present work was funded by the European Research Council in the framework of the HORIZON ERC-2022-COG project "Building a space Revolution: Electric Air-breathing Technology for High-atmosphere Exploration (BREATHE)", grant number 101088694, CUP n. J53C23001840006. Views and opinions expressed are, however, those of the authors only and do not necessarily reflect those of the European Research Council. Neither the European Union nor the granting authority can be held responsible for them.

### References

- [1] T. Andreussi, E. Ferrato, and V. Giannetti, "A review of air-breathing electric propulsion: from mission studies to technology verification," *Journal of Electric Propulsion*, vol. 1, no. 1, pp. 1–57, 2022.
- [2] V. Giannetti, E. Ferrato, and T. Andreussi, "On the critical parameters for feasibility and advantage of air-breathing electric propulsion systems," *Acta Astronautica*, vol. 220, pp. 345–355, 2024.
- [3] V. Pessina, M. Smirnova, and J. Schein, "Numerical framework for the development of atmosphere-breathing elec-

- tric propulsion for earth and mars atmosphere,” *Journal of Electric Propulsion*, vol. 3, no. 1, p. 28, 2024.
- [4] E. Ferrato, V. Giannetti, F. Califano, and T. Andreussi, “Atmospheric propellant fed hall thruster discharges: 0d-hybrid model and experimental results,” *Plasma Sources Science and Technology*, vol. 31, no. 7, p. 075003, 2022.
- [5] A. A. Sorokin, L. A. Shmaenok, S. V. Bobashev, B. Möbus, M. Richter, and G. Ulm, “Measurements of electron-impact ionization cross sections of argon, krypton, and xenon by comparison with photoionization,” *Phys. Rev. A*, vol. 61, p. 022723, 2000.
- [6] V. Hruby, K. Hohman, and J. Szabo, “Air breathing hall effect thruster design studies and experiments,” in *37th International Electric Propulsion Conference, Boston, Massachusetts, IEPC-2022-446*. <https://www.electricrocket.org/index.php>, 2022.
- [7] T. Andreussi, B. Moriconi, E. Ferrato, and V. Giannetti, “The breathe laboratory: A novel verification approach for air-breathing electric propulsion iepe-2024-384,” in *International Electric Propulsion Conference*, 2024.
- [8] F. Romanò, T. Binder, G. H. Herdrich, S. Fasoulas, and T. Schönherr, “Air-intake design investigation for an air-breathing electric propulsion system iepe-2015-90524 / ists-2015,” in *International Electric Propulsion Conference*, 2015.
- [9] G. A. Bird, *Molecular gas dynamics and the direct simulation of gas flows*. Oxford university press, 1994.
- [10] Y. Li, X. Chen, L. Wang, L. Guo, and Y. Li, “Molecular flow transmission probabilities of any regular polygon tubes,” *Vacuum*, vol. 92, pp. 81–84, 2013.
- [11] S. Barral, G. Cifali, R. Albertoni, M. Andrenucci, and L. Walpot, “Conceptual design of an air-breathing electric propulsion system,” *34th International Electric Propulsion Conference, Kobe, Japan, IEPC-2015-271*, 2015.
- [12] U. of Toronto. Institute of Aerophysics, D. Rothe, and J. DeLeeuw, *Numerical Solution for the Free-Molecule Impact-Pressure Probe Relations for Tubes of Arbitrary Length*, 1962.
- [13] R. P. Iczkowski, J. L. Margrave, and S. M. Robinson, “Effusion of gases through conical orifices,” *The Journal of Physical Chemistry*, vol. 67, no. 2, pp. 229–233, 1963.
- [14] T. Binder, P. C. Boldini, F. Romano, G. Herdrich, and S. Fasoulas, “Transmission probabilities of rarefied flows in the application of atmosphere-breathing electric propulsion,” vol. 1786, 11 2016, p. 190011.